Polymer Journal (2016) 48, 991–997

www.nature.com/pj

ORIGINAL ARTICLE

Dilute solution properties of poly(di-*tert*-butyl fumarate)

Nozomi Awazu, Takuya Komatsubara, Masashi Osa[1], Takenao Yoshizaki and Jiro Shimada

The mean-square radius of gyration $\langle S^2 \rangle$ and second virial coefficient A_2 are determined from static light scattering (LS) measurements for six samples of poly(di-*tert*-butyl fumarate) (PDtBF) for a range of weight-average molecular weight M_w from 4.35×10^4 to 1.73×10^5 in tetrahydrofuran at 30.0 °C. The intrinsic viscosity $[\eta]$ and translational diffusion coefficient D are also determined from viscosity and dynamic LS measurements for those samples under the same solvent conditions. From a simultaneous analysis of $\langle S^2 \rangle$ and A_2 based on the Kratky–Porod (KP) wormlike chain with excluded volume, the stiffness parameter λ^{-1} and the reduced excluded-volume strength λB are determined to be 350 Å and 0.024, respectively, where we assume the shift factor M_L for PDtBF to be 101 $Å^{-1}$ on the analogy of the main-chain structure of poly(diisopropyl fumarate) previously studied. For PDtBF with such a large λ^{-1}, it is found that the intramolecular excluded-volume effect for $\langle S^2 \rangle$ is negligibly small in the range of M_w examined. As for $[\eta]$ and D, their behavior may be well explained by the corresponding KP theories using the model parameter values consistent with those determined from $\langle S^2 \rangle$ and A_2, and the intramolecular excluded-volume effect for them can be ignored, as in the case of $\langle S^2 \rangle$.
Polymer Journal (2016) **48,** 991–997; doi:10.1038/pj.2016.63; published online 29 June 2016

INTRODUCTION

Recently, we conducted a study of the dilute solution properties of poly(diisopropyl fumarate) (PDiPF), which has ester isopropyl groups on every main-chain carbon atom, by determining its mean-square radius of gyration $\langle S^2 \rangle$, second virial coefficient A_2, intrinsic viscosity $[\eta]$ and translational diffusion coefficient D in tetrahydrofuran (THF) at 30.0 °C (good solvent).[1,2] Because of the steric hindrance of the bulky substituents preventing internal rotations around the main-chain C-C bonds, the PDiPF chain was predicted to be stiffer than common vinyl polymer chains having substituents on every other main-chain carbon atom.[3–5] From a simultaneous analysis of the experimental results for $\langle S^2 \rangle$ and A_2 based on the Kratky–Porod (KP) wormlike chain model[6,7] with a consideration of the intramolecular and intermolecular excluded-volume effects, the values of the stiffness parameter λ^{-1}, the shift factor M_L as defined as the molecular weight per unit contour length of the KP chain and the reduced excluded-volume strength[7] λB have been determined to be 113 Å, 89 $Å^{-1}$ and 0.097, respectively.[1] It has then been concluded from the value of λ^{-1} so determined that the PDiPF chain is stiffer than typical flexible polymers, such as atactic polystyrene ($\lambda^{-1} = 20.6$ Å),[7,8] as was expected. For $[\eta]$ and D (or the hydrodynamic radius R_H) of PDiPF, it has been shown that the experimental values agree well with the corresponding perturbed KP theory ones using the model parameter values consistent with the above ones determined from $\langle S^2 \rangle$ and A_2.[2]

Poly(di-*tert*-butyl fumarate) (PDtBF) with ester *tert*-butyl groups on every main-chain carbon atom belongs to the same category as PDiPF. Because the ester *tert*-butyl group of PDtBF is bulkier than the ester isopropyl group of PDiPF, the hindrance to the internal rotations is considered to be greater in the PDtBF chain than in the PDiPF one. Therefore, the former is expected to be still stiffer than the latter. In order to confirm this expectation, in the present study, we make a study of the dilute solution properties of PDtBF. We determine $\langle S^2 \rangle$, A_2, $[\eta]$ and D for PDtBF under the same solvent condition as in the case of PDiPF and evaluate λ^{-1} for PDtBF from analyses of the experimental data based on the KP model.

The analyses of $\langle S^2 \rangle$, $[\eta]$ and R_H of a semiflexible polymer in a good solvent require a comment. If its λ^{-1} is large and its weight-average molecular weight M_w is not very high, as in the case of typical semiflexible polymers with large λ^{-1} such as poly(*n*-hexyl isocyanate) with $\lambda^{-1} = 840$ Å,[9] then the intramolecular excluded-volume effect on those quantities may be negligibly small. In the previous case of PDiPF,[1,2] however, the value 113 Å of λ^{-1} is not large enough to ignore the effect in the range of M_w examined. Because there is currently no available information regarding the stiffness of the PDtBF chain, the analyses of $\langle S^2 \rangle$, $[\eta]$ and R_H of PDtBF should be carried out with the consideration of possible intramolecular excluded-volume effects. Therefore, we first analyze $\langle S^2 \rangle$ and A_2 of PDtBF simultaneously on the basis of the quasi-two-parameter (QTP) scheme[7,10–12] for the intramolecular excluded-volume effect and also the Yamakawa theory[7,13] of A_2 for the intermolecular excluded-volume effect. From the analysis, we determine the values of λ^{-1} and λB for PDtBF, with the value of M_L for PDtBF estimated by analogy with that for PDiPF. Then we compare the experimental data for $[\eta]$ and D with the corresponding KP theories combined with the QTP scheme, to ascertain the validity of the model parameter values determined from $\langle S^2 \rangle$ and A_2.

Department of Polymer Chemistry, Kyoto University, Kyoto, Japan
[1]Current address: Department of Chemistry, Aichi University of Education, 1 Hirosawa Igaya-cho, Kariya 448-8542, Japan.
Correspondence: Dr M Osa, Department of Chemistry, Aichi University of Education, Kariya 448-8542, Japan.
E-mail: mosa@auecc.aichi-edu.ac.jp
Received 1 February 2016; revised 11 April 2016; accepted 10 May 2016; published online 29 June 2016

EXPERIMENTAL PROCEDURE

Materials

The original PDtBF samples were synthesized by the radical polymerization of di-*tert*-butyl fumarate (DtBF), according to the procedure described by Otsu *et al.*[14] and Crivello and Shim.[15] Polymerization was carried out in benzene using dimethyl 2,2'-azobis(isobutyrate) (Wako Pure Chemical Industries, Ltd, Osaka, Japan) as an initiator under dry nitrogen at 60 °C for 24 h. The monomer DtBF was synthesized by the reaction of fumaryl chloride (Wako Pure Chemical Industries) with potassium *tert*-butoxide (Wako Pure Chemical Industries) in *tert*-butanol at reflux for 4 h. The synthesized PDtBF samples were purified by reprecipitation from benzene solutions into methanol and subsequently separated into fractions with narrow molecular weight distribution by fractional precipitation using toluene as a solvent and methanol as a precipitant. The six prepared test samples were freeze-dried from their benzene solutions.

The ratios of M_w to the number-average molecular weight M_n for all of the samples were determined from analytical gel permeation chromatography using THF as an eluent and standard polystyrene samples (Tosoh Corporation, Tokyo, Japan) as reference standards.

The THF solvent used for static light scattering (SLS), dynamic light scattering (DLS) and viscosity measurements was purified by distillation after refluxing over sodium. The THF solvent used for analytical gel permeation chromatography was of reagent grade.

Static light scattering

SLS measurements were carried out to determine M_w and A_2 for the six test samples and $\langle S^2\rangle$ for four test samples with $M_w > 7\times10^4$, in THF at 30.0 °C. The apparatus employed for the SLS measurements was the same as that used in the previous study for PDiPF.[1] The wavelength of the incident light was 436 nm. For each sample, at six different concentrations and at scattering angles θ ranging from 30.0 to 142.5°, the scattered light intensity was measured. We treated the obtained data by using the Berry square-root plot.[16] For all of the samples, the degree of depolarization was negligibly small, so that corrections for the optical anisotropy were unnecessary.

The most concentrated solution of each sample was prepared gravimetrically and then stirred continuously in the dark at room temperature for 2 days, to ensure homogeneity. For optical purification, the solution was filtered through a Teflon membrane Fluoropore (Sumitomo Electric Industries, Ltd, Osaka, Japan) with a pore size of 0.10 μm. To obtain the solutions of lower concentrations, the most concentrated solution was successively diluted. The polymer mass concentrations c were converted from the weight concentrations by using the densities of each solution, which were calculated with the partial specific volumes ν_2 of the samples and with the density ρ_0 of the solvent THF. ν_2 and ρ_0 were measured using an oscillating U-tube density meter DMA5000 (Anton-Paar, Graz, Austria). For all of the samples, the values of ν_2 in THF at 30.0 °C are 0.876 $cm^3\,g^{-1}$. The value of ρ_0 for THF at 30.0 °C is 0.8751 $g\,cm^{-3}$.

The measurements of the refractive index increment $\partial n/\partial c$ were carried out by using the same apparatus as in the previous study for PDiPF.[1] For all of the samples, the values of $\partial n/\partial c$ in THF at 30.0 °C and at the wavelength of 436 nm are 0.0770 $cm^3\,g^{-1}$. The refractive index n_0 of THF at 30.0 °C and at the wavelength of 436 nm is 1.4108.[1]

Viscosity

Viscosity measurements were carried out for the six samples in THF at 30.0 °C, using a conventional capillary viscometer of the Ubbelohde type, to determine $[\eta]$ and the Huggins coefficient k' of the samples. The details of the procedures of the measurements, data collection and data processing have been described in a previous study.[2]

Dynamic light scattering

DLS measurements were carried out to determine D for all of the samples except PDtBF4 in THF at 30.0 °C. The apparatus employed for the DLS measurements was the same as that used in the previous study for PDiPF.[2] The wavelength of the incident light was 532 nm. For each sample, at 3–6 concentrations and at scattering angles θ ranging from 30 to 50°, the normalized autocorrelation function $g^{(2)}(t)$ of the scattered light intensity was measured. The preparation and the optical purification of the solutions were made in the same manner as in the cases of the SLS measurements. The details of the data acquisition and data processing have been described in previous studies.[2,17,18] The values of n_0 at the wavelength of 532 nm and of the viscosity coefficient η_0 for THF at 30.0 °C are 1.4045 and 0.439_7 cP, respectively.[2]

RESULTS

The values of M_w determined from SLS measurements in THF at 30.0 °C and M_w/M_n from analytical gel permeation chromatography for all the six PDtBF samples are listed in the second and third columns of Table 1, respectively. In the fourth column of Table 1 are listed the values of the weight-average number of repeat units n_w calculated by the following equation,

$$n_w = 2M_w/M_0 \tag{1}$$

where M_0 is the molecular weight of the monomer unit. We note that the values of M_0 are 228 and 200 for PDtBF and PDiPF, respectively. We also note that the range of M_w (and also n_w) for PDtBF is somewhat narrower than that for the PDiPF previously investigated,[1,2] probably because the applied polymerization time for the former samples was shorter than that for the latter ones.

As for the stereochemical compositions of PDtBF prepared by radical polymerization, Yoshioka *et al.*[19,20] have reported that the fraction f_r of *racemo* diads depends on the polymerization temperature and that the value of f_r for the PDtBF samples synthesized at 60 °C is 0.14. Therefore, we think that the values of f_r for the present PDtBF samples are approximately 0.14. This value is not far from the f_r value 0.22 for the PDiPF samples that have previously[1,2] been studied. Here it should be noted that if vicinal substituents joined to a pair of adjacent backbone carbon atoms (diad) in a PDtBF (or PDiPF) chain are located on opposite sides of a plane containing all of the backbone carbon atoms of the chain in the planer trans conformation, then the diad is called *meso*; otherwise, the diad is called *racemo*.[21]

Mean-square radius of gyration $\langle S^2\rangle$

The values of $\langle S^2\rangle$ determined from the SLS measurements for the PDtBF samples in THF at 30.0 °C are listed in the fifth column of Table 1. In the table, the values of $\langle S^2\rangle$ for the samples PDtBF4 and PDtBF5 have been excluded because the values of $\langle S^2\rangle$ for these samples are too small to determine accurately by the SLS measurements.

Figure 1 shows the double-logarithmic plots of the ratio of $\langle S^2\rangle$ ($\langle S^2\rangle$ in Å^2) to n_w against n_w. The unfilled circles represent the present experimental data for PDtBF in THF at 30.0 °C. The solid and dashed curves represent the theoretical values for the KP chain with and without the excluded volume, respectively, which are discussed in the Discussion section. $\langle S^2\rangle/n_w$ for PDtBF increases monotonically with increasing n_w.

Table 1 Values of M_w/M_n and n_w and the results of the SLS measurements for poly(di-*tert*-butyl fumarate) in tetrahydrofuran at 30.0 °C

Sample	M_w	M_w/M_n	n_w	$10^{-4}\langle S^2\rangle$ (Å^2)	$10^4 A_2$ ($cm^3\,mol\,g^{-2}$)
PDtBF4	4.35×10^4	1.14	382	—	3.31
PDtBF5	4.73×10^4	1.15	415	—	3.47
PDtBF8	7.98×10^4	1.17	700	2.58	2.88
PDtBF9	8.88×10^4	1.21	779	3.07	3.24
PDtBF15	1.46×10^5	1.22	1280	6.15	2.43
PDtBF17	1.73×10^5	1.24	1520	7.41	2.33

Abbreviations: PDtBF, poly(di-*tert*-butyl fumarate); SLS, static light scattering.

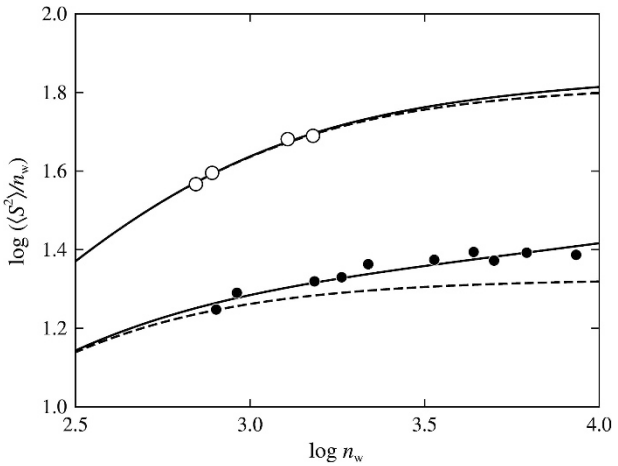

Figure 1 Double-logarithmic plots of $\langle S^2\rangle/n_w$ ($\langle S^2\rangle$ in Å^2) against n_w: (○) present data for PDtBF in THF at 30.0 °C; (●) previous data for PDiPF in THF at 30.0 °C.[1] The solid and dashed curves represent the best-fit theoretical values for the KP chain with and without the excluded volume, respectively.

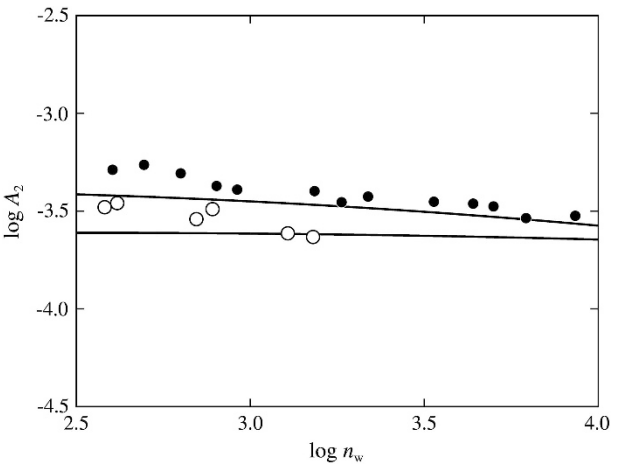

Figure 2 Double-logarithmic plots of A_2 (in cm^3 mol g^{-2}) against n_w. All of the symbols have the same meaning as those in Figure 1. The solid curves represent the theoretical values for the KP chain without the effects of chain ends (see the text).

For comparison, the previous data for PDiPF in THF at 30.0 °C[1] are also plotted in the figure (filled circles). The values of $\langle S^2\rangle/n_w$ for PDtBF are definitely larger than those for PDiPF, indicating that the average dimension of the polymer chains for PDtBF is much larger than that for PDiPF probably because of a remarkable difference in the chain stiffness between the two polymers.

Second virial coefficient A_2

The values of A_2 determined from the SLS measurements in THF at 30.0 °C for all of the PDtBF samples are listed in the sixth column of Table 1.

Figure 2 shows the double-logarithmic plots of A_2 (in cm^3 mol g^{-2}) against n_w for PDtBF in THF at 30.0 °C (unfilled circles). It includes the previous data for PDiPF in THF at 30.0 °C[1] (filled circles), for comparison. The solid curves represent the theoretical values for the KP chain without the effects of the chain ends, which are discussed in the Discussion section. The values of A_2 for PDtBF are smaller than those for PDiPF, implying that THF at 30.0 °C is not as good a solvent for PDtBF as it is for PDiPF.

Table 2 Results of the viscosity and DLS measurements for poly (di-*tert*-butyl fumarate) in tetrahydrofuran at 30.0 °C

Sample	*[η] (dl g^{-1})*	k′	*10^7D (cm^2 s^{-1})*	*$k_D^{(LS)}$ (cm^3 g^{-1})*	*R_H (Å)*
PDtBF4	0.375	0.51	—	—	—
PDtBF5	0.378	0.51	7.09	11	71
PDtBF8	0.670	0.50	4.89	21	103
PDtBF9	0.775	0.38	4.23	32	119
PDtBF15	1.07	0.47	3.36	38	150
PDtBF17	1.27	0.47	3.01	30	168

Abbreviations: PDtBF, poly(di-*tert*-butyl fumarate); DLS, dynamic light scattering.

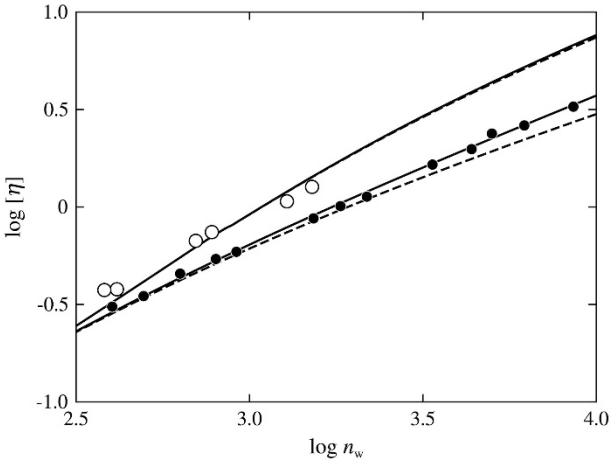

Figure 3 Double-logarithmic plots of $[\eta]$ (in dl g^{-1}) against n_w: (○) present data for PDtBF in THF at 30.0 °C; (●) previous data for PDiPF in THF at 30.0 °C.[2] The solid and dashed curves represent the best-fit theoretical values for the KP chain with and without the excluded volume, respectively.

Intrinsic viscosity $[\eta]$

The values of $[\eta]$ and k' determined from the viscosity measurements in THF at 30.0 °C for all of the PDtBF samples are listed in the second and third columns of Table 2. The values of k' for PDtBF are larger than those for PDiPF ($k' = 0.3$–0.4) previously reported.[2] This result is consistent with the fact that THF at 30.0 °C is a better solvent for PDiPF than it is for PDtBF, as deduced from the above-mentioned result of A_2.

Figure 3 shows the double-logarithmic plots of $[\eta]$ (in dl g^{-1}) against n_w for PDtBF in THF at 30.0 °C (unfilled circles). For comparison, it includes the previous results for PDiPF in THF at 30.0 °C[2] (filled circles). All of the curves have the same meaning as those in Figure 1. As in the case of $\langle S^2\rangle$, the values of $[\eta]$ for PDtBF are appreciably larger than those for PDiPF, indicating that the effective hydrodynamic (molar) volume is much larger for PDtBF than it is for PDiPF, probably because of a large difference in the chain stiffness between the two polymers.

Translational diffusion coefficient D and hydrodynamic radius R_H

The values of D and $k_D^{(LS)}$ determined from the DLS measurements in THF at 30.0 °C for all of the PDtBF samples except PDtBF4 are listed in the fourth and fifth columns of Table 2. We note that $k_D^{(LS)}$ is concerned with the coefficient of the concentration c in the expansion

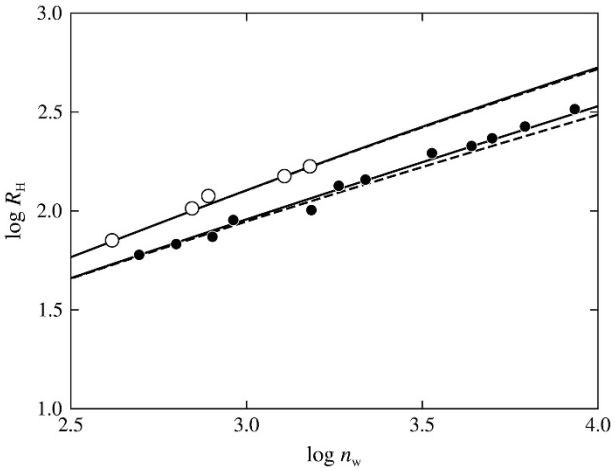

Figure 4 Double-logarithmic plots of R_H (in Å) against n_w. All of the symbols have the same meaning as those in Figure 3. The solid and dashed curves represent the best-fit theoretical values for the KP chain with and without the excluded volume, respectively.

of the apparent diffusion coefficient $D^{(LS)}(c)$ at finite c.[18] In the last column of Table 2 are also listed the values of the hydrodynamic radius R_H calculated from the defining equation

$$R_H = k_B T/6\pi\eta_0 D \tag{2}$$

where k_B is the Boltzmann constant and T is the absolute temperature.

In Figure 4, R_H (in Å) is double-logarithmically plotted against n_w for PDtBF in THF at 30.0 °C (unfilled circles). For comparison, the previous results for PDiPF in THF at 30.0 °C[2] are also included in the figure (filled circles). All of the curves have the same meaning as those in Figure 1. As in the cases of $\langle S^2\rangle$ and $[\eta]$, the values of R_H for PDtBF are larger than those for PDiPF.

DISCUSSION

Analyses of $\langle S^2\rangle$ and A_2 on the basis of the KP model

In this section, we simultaneously analyze the present data of $\langle S^2\rangle$ and A_2 for PDtBF on the basis of the KP model with consideration of both the intramolecular and intermolecular excluded-volume effects and determine the model parameter values for PDtBF. The KP chain[6,7] itself is an elastic wire model that possesses only a bending energy and may be characterized by the stiffness parameter λ^{-1} having the dimension of length. The KP chain model is a special case of the helical wormlike (HW) chain[7] model, which is a more general polymer chain model having a torsional energy in addition to the bending energy.

For the KP chain of total contour length L, $\langle S^2\rangle$ may be written in the form,

$$\langle S^2\rangle = \langle S^2\rangle_0 \alpha_S^2 \tag{3}$$

where $\langle S^2\rangle_0$ is the unperturbed mean-square radius of gyration given as a function of λ^{-1} and L by equation 5 of Nakatsuji *et al.*[1,7,22] In Equation 3, α_S is the gyration-radius expansion factor concerned with the intramolecular excluded-volume effect. In the framework of the QTP scheme,[7,10–12] α_S is a function only of the intramolecular scaled excluded-volume parameter $\tilde{z}$, and for the function of α_S, we usually use the Domb–Barrett equation[23] given by equation 6 of Nakatsuji *et al.*[1] The parameter $\tilde{z}$ is defined as a product of a function $3/4 \times K(\lambda L)$ and the conventional excluded-volume parameter z defined in the two-parameter (TP) scheme.[7,24] The function $K(\lambda L)$ of the reduced contour length λL represents the effects of the chain stiffness on the intramolecular excluded-volume effect and is given by equation 8 of Nakatsuji *et al.*[1] The parameter z may be written by using the reduced excluded-volume strength λB and λL, as obtained with equation 9 of Nakatsuji *et al.*[1] The excluded-volume strength B is related to the binary-cluster integral β of the beads, which are arrayed along the KP chain in order to incorporate the excluded volume into the chain.[7]

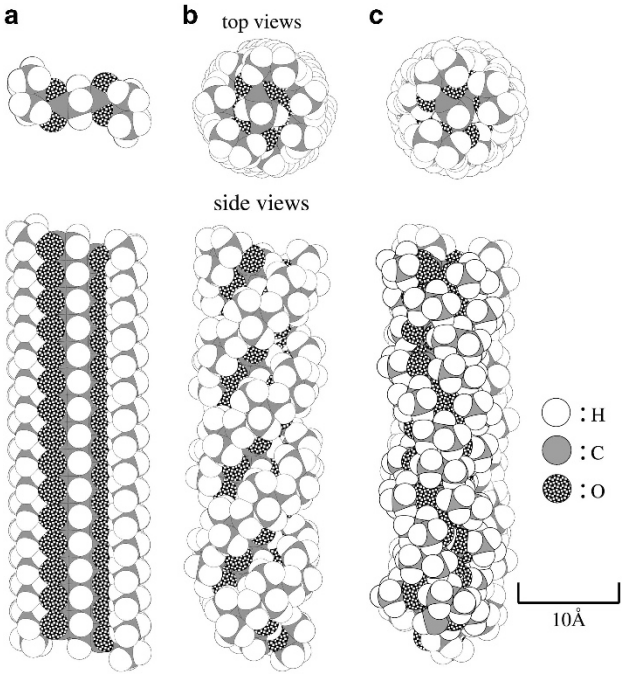

Figure 5 Schematic drawing of the chain conformations of PDtBF with $f_r = 0$, where all of the atoms are depicted by spheres with diameters corresponding to the van der Walls radii: (**a**) the planar *trans* conformation with $\phi = 0$; (**b**) the helical conformation with $\phi = 30°$; (**c**) the helical conformation with $\phi = 60°$.

In the theory by Yamakawa *et al.*,[7,13] A_2 of the KP chain may then be written in the form,

$$A_2 = A_2^{(HW)} + A_2^{(E)} \tag{4}$$

where $A_2^{(HW)}$ is a part of A_2 without the effects of the chain ends and $A_2^{(E)}$ represents the contribution of the effects of the chain ends. The superscript (HW) attached to the first term indicates that the theory is originally constructed on the basis of the HW chain. For a KP chain of total length L with an excluded-volume strength B, $A_2^{(HW)}$ may be given as a function of λ^{-1}, M_L, λB and λL by using equation 13 together with equations 6–9 and 14–18 of Nakatsuji *et al.*[1] We note that the second term $A_2^{(E)}$ in Equation 4 rapidly decreases to 0 with increasing molecular weight M and may be neglected for $M \gtrsim 10^5$ for all of the polymer-solvent systems examined so far.[7,25–29]

To compare the above-mentioned KP theoretical values of $\langle S^2\rangle$ and A_2 calculated as functions of L with the experimental ones as functions of M or the number of repeat units n in the polymer chain, L is related to M or n by

$$L = M/M_L = nM_0/2M_L \tag{5}$$

with the shift factor M_L. In this manner, we may in principle determine the three parameters λ^{-1}, M_L and λB by simultaneous curve fitting of the KP theoretical values to the experimental data for $\langle S^2\rangle$ and A_2.

Unfortunately, however, the range 382–1520 of n_w for the present PDtBF samples is not sufficiently wide to unambiguously determine all of the KP model parameters from such an analysis. In order to reduce the number of the parameters to be determined, we assume the value of M_L for PDtBF to be 101 Å^{-1}. This value has been calculated by assuming that the ratio of the value of M_L for PDtBF to that for PDiPF (89 Å^{-1})[1] is equal to the ratio of the value of M_0 for the former (228) to that for the latter (200). To the best of our knowledge, there are no available data for the crystal structure of PDtBF. Therefore, in order to confirm whether the above-assigned value of 101 Å^{-1} for M_L is reasonable or not, we estimate M_L on the basis of the chain conformations of PDtBF. In Figure 5a, the PDtBF chain (with $n=30$ and $f_r=0$) in the planar *trans* conformation (with an internal rotation angle ϕ of 0° and with a bond angle of 109°) is schematically illustrated, whose M_L may be estimated as 95 Å^{-1}. The M_L value for a polymer chain in a helical conformation generally becomes larger than that for the chain in the planar *trans* conformation, so the (true) M_L value for the PDtBF chain may be larger than 95 Å^{-1}. For the PDtBF chain (with $n=30$ and $f_r=0$) in helical conformations, we demonstrate two chains having fixed $\phi=30°$ and 60°, which are schematically illustrated in Figures 5b and c, respectively. The values of M_L are estimated to be 96 and 100 Å^{-1} for $\phi=30°$ and 60°, respectively. These values do not significantly differ from 95 Å^{-1} (and also from 101 Å^{-1}). In order to investigate the preferred chain conformation of PDtBF, the PDtBF chains for $\phi=0°$, 30° and 60° were generated with AMBER12[30] using a generalized amber force field (gaff). Then it was found that the chain conformation of PDtBF with the lowest total conformational energy (in vacuum) is in the 10_1 helical conformation, where the rotation angles associated with two successive main-chain bonds are alternately 0° and 60°. The value of M_L for this 10_1 helical conformation is evaluated as 95 Å^{-1}. Considering these facts, the value 101 Å^{-1} of M_L assigned above is consistent with those estimated on the basis of the chain conformations of PDtBF. Thus we adopt the value 101 Å^{-1} of M_L and then attempt to determine the remaining two model parameters, λ^{-1} and λB, from a simultaneous comparison of the KP theories of $\langle S^2\rangle$ and A_2 with the experimental data.

In Figures 1 and 2, the solid curves associated with the present data points for PDtBF represent the best-fit KP theory values of $\langle S^2\rangle$ and those of A_2 without a consideration of the effects of chain ends, that is, $A_2^{(HW)}$, respectively, where these theoretical values have been calculated with $\lambda^{-1}=350$ Å and $\lambda B=0.024$ along with the above-mentioned value 101 Å^{-1} of M_L. We note that the determination errors in the values of λ^{-1} and λB for PDtBF are evaluated as ±7% and ±8%, respectively, at most. In the figures, the solid curves associated with the data points for PDiPF represent the best-fit KP theory values calculated in the same manner as in the case of PDtBF, with the model parameter values previously determined[1] ($\lambda^{-1}=113$ Å, $M_L=89$ Å^{-1} and $\lambda B=0.097$). It is seen from the figures that for PDtBF the theoretical values may well reproduce the experimental values of $\langle S^2\rangle$ over the whole range of n_w examined and those of A_2 in the range of $n_w \gtrsim 10^3$, where the effects of the chain ends may be negligibly small. The value 350 Å of λ^{-1} determined for PDtBF is appreciably larger than that for PDiPF, as is expected from their chemical structures. Therefore, it may be concluded that the difference in the substituents between PDtBF and PDiPF, that is, ester *tert*-butyl group and ester isopropyl one, has a great influence on the chain stiffness and also on the average chain dimensions of the two polymers. In Figure 2, the data points for each polymer are seen to deviate progressively upward from the theoretical curve with decreasing n_w for $n_w \lesssim 10^3$, because of the effects of the chain ends ($A_2^{(E)}$).

Concerning the side-chain group dependence of the average chain dimension, it is pertinent to refer to the literature data[31–33] for poly (methacrylic acid) derivatives (that is, polymethacrylates). The data show that an increase in size of side-chain groups of the polymethacrylates is accompanied by an increase in the coil-limiting value C_∞ of the characteristic ratio, that is, an increase in the average chain dimension. This trend is consistent with the results obtained for PDiPF and PDtBF.

In Figure 1, the theoretical values of $\langle S^2\rangle_0$ (dashed curves) for the respective polymers, calculated with the same model parameter values of λ^{-1} and M_L as those mentioned above, are also shown. It is seen from the figure that the present data points for PDtBF agree with the theoretical values of $\langle S^2\rangle_0$, as well as those of $\langle S^2\rangle$ (solid curve), for the whole range of n_w examined. On the other hand, the data points for PDiPF are seen to deviate progressively upward from the theoretical $\langle S^2\rangle_0$ with increasing n_w. These results indicate that the intramolecular excluded-volume effect may be ignored for PDtBF in the range of n_w examined, while the effect cannot be ignored for PDiPF because the PDiPF chain is much more flexible than the PDtBF one.

Analysis of [η] on the basis of the KP model

Next we proceed to analyze the data for $[\eta]$ on the basis of the unperturbed KP cylinder model[7,34,35] combined with the QTP theory.[7,10–12]

For the perturbed KP cylinder model with excluded volume, $[\eta]$ may be expressed as

$$[\eta] = [\eta]_0 \alpha_\eta^3 \tag{6}$$

where $[\eta]_0$ is the intrinsic viscosity for the unperturbed KP cylinder model of total length L and diameter d and may be given as a function of λ^{-1}, λL and the reduced diameter λd by using equation 6.89 with equation 6.90 of Yamakawa and Yoshizaki[7] for $\lambda L \geqslant 2.278$ and equation 6.91 with equations 6.92 and 6.94 of Yamakawa and Yoshizaki[7] for $\lambda L < 2.278$. In Equation 6, α_η is the viscosity-radius expansion factor. In the framework of the QTP scheme,[7,10–12] α_η is a function only of $\tilde{z}$. As usual,[7] for α_η, we adopt the Barrett equation[36] given by equation 17 of Nakatsuji *et al*.[2]

On the basis of the theory, the perturbed KP theory value of $[\eta]$ may be calculated as a function of M or n for a given set of values of the four model parameters λ^{-1}, M_L, λB and d. Namely, we can determine the parameters for PDtBF from curve fitting to the experiment data for $[\eta]$. However, as seen from Figure 3, the increase in $[\eta]$ for PDtBF with increasing n_w is monotonic, and the plot does not show any prominent feature such as an S-shaped curve, which was observed for poly(*n*-hexyl isocyanate).[9] Therefore, it is difficult to determine all of the parameters from the curve fitting. Thus we assume values of 350 Å and 0.024 for λ^{-1} and λB, respectively, as determined above from the analyses of $\langle S^2\rangle$ and A_2 and then determine the two parameters M_L and d, as done in the case of PDiPF.[2]

In Figure 3, the solid curve associated with the data points for PDtBF represents the best-fit perturbed KP theory values for PDtBF calculated with $M_L=123$ Å^{-1} and $d=17$ Å and the above-mentioned values of λ^{-1} and λB. In the figure, the solid curve associated with the data points for PDiPF represents the best-fit perturbed KP theory values for PDiPF, calculated with the model parameter values previously determined[2] for PDiPF ($\lambda^{-1}=113$ Å, $M_L=92$ Å^{-1}, $d=15$ Å and $\lambda B=0.097$). The experimental values are in good agreement with those of the perturbed KP theory calculated with the model parameter values, which are consistent with those determined from $\langle S^2\rangle$ and A_2 for each polymer. A value of 17 Å for d for

PDtBF is close to the value of 15 Å for PDiPF, indicating that the difference in the substituents between the two polymers has no significant effect on the (hydrodynamic) chain thickness of them but remarkably affects the chain stiffness.

Analysis of R_H on the basis of the KP model

In this subsection, we analyze the data for R_H on the basis of the unperturbed KP cylinder model[7,37,38] combined with the QTP theory.[7,10–12]

For the perturbed KP cylinder model with excluded volume, R_H may be expressed as

$$R_H = R_{H,0}\alpha_H \tag{7}$$

where $R_{H,0}$ is the hydrodynamic radius for the unperturbed KP cylinder model of total length L and diameter d and may be given as a function of λ^{-1}, λL, and λd by using equations 6.41—6.43 with equations 6.22 and 6.23 of Yamakawa and Yoshizaki.[7] In Equation 7, α_H is the hydrodynamic-radius expansion factor. In the framework of the QTP scheme,[7,10–12] α_H is also a function only of $\tilde{z}$ and may be expressed as a product of $\alpha_{H,0}$, for which we usually use the Barrett equation[39] given by equation 24 of Nakatsuji *et al.*,[2] and h_H, which represents a possible effect of the fluctuating hydrodynamic interaction on α_H and is given by equation 25 of Nakatsuji *et al.*[2,7,40]

The perturbed KP theory of R_H may also be calculated as a function of M or n for a given set of values of the four model parameters λ^{-1}, M_L, λB and d. As in the case of $[\eta]$, we assume the values of 350 Å and 0.024 for λ^{-1} and λB, respectively, and determine the two parameters M_L and d from curve fitting to the experimental data for R_H.

In Figure 4, the solid curve associated with the data points for PDtBF represents the best-fit perturbed KP theory values for PDtBF, as calculated with $M_L = 80$ Å^{-1} and $d = 18$ Å and the above-mentioned values of λ^{-1} and λB. In the figure, the solid curve associated with the data points for PDiPF represents the best-fit perturbed KP theory values for PDiPF, as calculated with the model parameter values previously determined[2] for PDiPF ($\lambda^{-1} = 113$ Å, $M_L = 81$ Å^{-1}, $d = 16$ Å and $\lambda B = 0.097$). The theoretical values may well explain the behavior of the experimental data points for each polymer. A value of 80 Å^{-1} for M_L determined from R_H for PDtBF is relatively small compared with the 123 Å^{-1} determined from $[\eta]$ and the 101 Å^{-1} used in the analyses of $\langle S^2\rangle$ and A_2. This difference may be attributed to the discrepancy between the theoretical and experimental values of the coil-limiting value Φ_∞ of the Flory–Fox factor and the coil-limiting value ρ_∞ of the ratio of $\langle S^2\rangle_0^{1/2}$ to $R_{H,0}$, as previously mentioned.[7,17] Taking account of this fact, we arrive at the conclusion that the unperturbed KP theory combined with the QTP theory may comprehensively explain the behavior of the experimental values for the four properties $\langle S^2\rangle$, A_2, $[\eta]$ and R_H for PDtBF as well as for PDiPF.

In Figure 4 (also in Figure 3), the dashed curves represent the unperturbed KP theory values calculated with the same model parameter values of λ^{-1}, M_L and d as those used in the calculations of the perturbed KP theory ones for the respective polymers. The present data points for PDtBF agree with the unperturbed KP theory values as well as the perturbed theory ones, indicating that the intramolecular excluded-volume effects on R_H (and $[\eta]$) of PDtBF may be ignored in the range of n_w examined, as in the case of $\langle S^2\rangle$. As for PDiPF, the experimental values and those of the perturbed KP theory are in good agreement with the unperturbed KP theory values for $n_w \lesssim 10^3$ but deviate progressively upward from the latter with increasing n_w for $n_w \gtrsim 10^3$ because of the intramolecular excluded-volume effect, as previously mentioned.[2]

CONCLUSION

We have determined $\langle S^2\rangle$, A_2, $[\eta]$ and D (and R_H) for PDtBF in THF at 30.0 °C in the range of M_w from 4.35×10^4 to 1.73×10^5. From the simultaneous analysis of $\langle S^2\rangle$ and A_2 on the basis of the corresponding KP theories with a consideration of both the intramolecular and intermolecular excluded-volume effects, λ^{-1} and λB for PDtBF have been determined, with M_L having been estimated by analogy with that for PDiPF. The value 350 Å of λ^{-1} determined for PDtBF is substantially larger than the value 113 Å for the PDiPF that was previously[1] studied, indicating that the difference in the substituents between the two polymers causes the remarkable difference in chain stiffness. It has been found that the PDtBF chain is so stiff that the intramolecular excluded-volume effect for $\langle S^2\rangle$ may be ignored in the range of M_w examined. As for $[\eta]$ and R_H, the data have been analyzed on the basis of the corresponding theories for the KP cylinder model combined with the QTP theory. It has been shown that the experimental values agree well with the KP theory values using the model parameter values consistent with those determined from $\langle S^2\rangle$ and A_2. It has also been shown that the intramolecular excluded-volume effects of $[\eta]$ and R_H for PDtBF may be ignored as in the case of $\langle S^2\rangle$.

CONFLICT OF INTEREST

The authors declare no conflict of interest.

ACKNOWLEDGEMENTS

This work was supported by JSPS KAKENHI Grant Number 22750111.

1 Nakatsuji, M., Hyakutake, M., Osa, M. & Yoshizaki, T. Mean-square radius of gyration and second virial coefficient of poly(diisopropyl fumarate) in dilute solution. *Polym. J.* **40**, 566–571 (2008).
2 Nakatsuji, M., Soutoku, K., Osa, M. & Yoshizaki, T. Transport coefficients of poly (diisopropyl fumarate) in dilute solution. *Polym. J.* **41**, 83–89 (2009).
3 Otsu, T., Minai, H., Toyoda, N. & Yasuhara, T. Radical high polymerization of dialkyl fumarates with bulky substituents leading to less-flexible rod-like polymers. *Makromol. Chem. Suppl.* **12**, 133–142 (1985).
4 Matsumoto, A., Tarui, T. & Otsu, T. Dilute solution properties of semiflexible poly (substituted methylenes): intrinsic viscosity of poly(diisopropyl fumarate) in benzene. *Macromolecules* **23**, 5102–5105 (1990).
5 Matsumoto, A. & Nakagawa, E. Evaluation of chain rigidity of poly(diisopropyl fumarate) from light scattering and viscosity in tetrahydrofuran. *Euro. Polym. J.* **35**, 2107–2113 (1999).
6 Kratky, O. & Porod, G. Röntgenuntersuchung gelöster fadenmoleküle. *Recl. Trav. Chim. Pays Bas* **68**, 1106–1122 (1949).
7 Yamakawa, H. & Yoshizaki, T. *Helical Wormlike Chains in Polymer Solutions*, 2nd edn. (Springer, Berlin, Germany, 2016).
8 Abe, F., Einaga, Y., Yoshizaki, T. & Yamakawa, H. Excluded-volume effects on the mean- square radius of gyration of oligo- and polystyrenes in dilute solutions. *Macromolecules* **26**, 1884–1890 (1993).
9 Murakami, H., Norisuye, T. & Fujita, H. Dimensional and hydrodynamic properties of poly(hexyl isocyanate) in hexane. *Macromolecules* **13**, 345–352 (1980).
10 Yamakawa, H. & Stockmayer, W. H. Statistical mechanics of wormlike chains. II. Excluded volume effects. *J. Chem. Phys.* **57**, 2843–2854 (1972).
11 Yamakawa, H. & Shimada, J. Stiffness and excluded-volume effects in polymer chains. *J. Chem. Phys.* **83**, 2607–2611 (1985).
12 Shimada, J. & Yamakawa, H. Statistical mechanics of helical worm-like chains. XV. Excluded-volume effects. *J. Chem. Phys.* **85**, 591–600 (1986).
13 Yamakawa, H. On the theory of the second virial coefficient for polymer chains. *Macromolecules* **25**, 1912–1916 (1992).
14 Otsu, T., Yasuhara, T., Shiraishi, K. & Mori, S. Radical high polymerization of di-*tert*-butyl fumarate and novel synthesis of high molecular weight poly(fumaric acid) from its polymer. *Polym. Bull.* **12**, 449 (1984).
15 Crivello, J. V. & Shim, S.-Y. Deep UV photoresists based on poly(di-*tert*-butyl fumarate). *J. Polym. Sci. Part A Polym. Chem.* **33**, 513–523 (1995).
16 Berry, G. C. Thermodynamic and conformational properties of polystyrene. I. Light-scattering studies on dilute solutions of linear polystyrenes. *J. Chem. Phys.*, **44**, 4550–4564 (1966).
17 Konishi, T., Yoshizaki, T. & Yamakawa, H. On the "universal constants" ρ and Φ of flexible polymers. *Macromolecules* **24**, 5614–5622 (1991).

18 Yamada, T., Yoshizaki, T. & Yamakawa, H. Transport coefficients of helical wormlike chains. 5. Translational diffusion coefficient of the touched-bead model and its application to oligo- and polystyrenes. *Macromolecules* **25**, 377–383 (1992).
19 Yoshioka, M., Matsumoto, A. & Otsu, T. *meso* and *racemo* additions in propagation for radical polymerization of dialkyl fumarates I. Stereoregularity of poly(dialkyl fumarate)s. *Polym. J.* **23**, 1191–1196 (1991).
20 Yoshioka, M., Matsumoto, A. & Otsu, T. *meso* and *racemo* additions in propagation for radical polymerization of dialkyl fumarates II. Determination of the absolute rate constants. *Polym. J.* **23**, 1249–1252 (1991).
21 Wang, X., Komoto, T., Ando, I. & Otsu, T. Stereochemical configuration of polyfumarates as studied by ^{13}C nuclear magnetic resonance spectroscopy. *Makromol. Chem.* **189**, 1845–1854 (1988).
22 Benoit, H. & Doty, P. Light scattering from non-gaussian chains. *J. Phys. Chem.* **57**, 958–963 (1953).
23 Domb, C. & Barrett, A. J. Universality approach to the expansion factor of a polymer chain. *Polymer* **17**, 179–184 (1976).
24 Yamakawa, H. *Modern Theory of Polymer Solutions* (Harper & Row, New York, USA, 1971). Its electronic edition is available online at the URL http://www.molsci.polym.kyoto-u.ac.jp/archives/redbook.pdf.
25 Kasabo, F., Kanematsu, T., Nakagawa, T., Sato, T. & Teramoto, A. Solution properties of cellulose tris(phenyl carbamate). 1. Characterization of the conformation and intermolecular interaction. *Macromolecules* **33**, 2748–2756 (2000).
26 Einaga, Y., Abe, F. & Yamakawa, H. Second virial coefficients of oligo- and polystyrenes. Effects of chain ends. *Macromolecules* **26**, 6243–6250 (1993).
27 Abe, F., Einaga, Y. & Yamakawa, H. Second virial coefficient of oligo- and poly(methyl methacrylate)s. Effects of chain stiffness and chain ends. *Macromolecules* **27**, 3262–3271 (1994).
28 Kamijo, M., Abe, F., Einaga, Y. & Yamakawa, H. Second virial coefficient of isotactic oligo- and poly(methyl methacrylate)s. Effects of chain stiffness and chain ends. *Macromolecules* **28**, 4159–4166 (1995).
29 Tokuhara, W., Osa, M., Yoshizaki, T. & Yamakawa, H. Second virial coefficient of oligo- and poly(α-methylstyrene)s. Effects of chain stiffness, chain ends, and three-segment interactions. *Macromolecules* **36**, 5311–5320 (2003).
30 Case, D. A., Darden, T. A., Cheatham, T. E. III, Simmerling, C. L., Wang, J., Duke, R. E., Luo, R., Walker, R. C., Zhang, W., Merz, K. M., Roberts, B., Hayik, S., Roitberg, A., Seabra, G., Swails, J., Götz, A. W., Kolossváry, I., Wong, K. F., Paesani, F., Vanicek, J., Wolf, R. M., Liu, J., Wu, X., Brozell, S. R., Steinbrecher, T., Gohlke, H., Cai, Q., Ye, X., Wang, J., Hsieh, M.-J., Cui, G., Roe, D. R., Mathews, D. H., Seetin, M. G., Salomon-Ferrer, R., Sagui, C., Babin, V., Luchko, T., Gusarov, S., Kovalenko, A. & Kollman, P. A. (2012) AMBER 12, University of California, San Francisco.
31 Zhongde, X., Hadjichristidis, N. & Fetters, L. Solution properties and chain dimensions of poly(*n*-alkyl methacrylates). *Macromolecules* **17**, 2303–2306 (1984).
32 Siakali-Kioulafa, E., Hadjichristidis, N. & Mays, J. Synthesis and solution properties of polymethacrylates with alicyclic side groups. *Macromolecules* **22**, 2059–2062 (1989).
33 Karandinos, A., Nan, S., Mays, J. & Hadjichristidis, N. Solution properties and unperturbed dimensions of stereoirregular poly(*tert*-butyl methacrylates). *Macromolecules* **24**, 2007–2010 (1991).
34 Yamakawa, H. & Fujii, M. Intrinsic viscosity of wormlike chains. Determination of the shift factor. *Macromolecules* **7**, 128–135 (1974).
35 Yamakawa, H. & Yoshizaki, T. Transport coefficients of helical wormlike chains. 3. Intrinsic viscosity. *Macromolecules* **13**, 633–643 (1980).
36 Barrett, A. J. Intrinsic viscosity and friction coefficients for an excluded volume polymer in the Kirkwood approximations. *Macromolecules* **17**, 1566–1572 (1984).
37 Yamakawa, H. & Fujii, M. Translational friction coefficient of wormlike chains. *Macromolecules* **6**, 407–415 (1973).
38 Yamakawa, H. & Yoshizaki, T. Transport coefficients of helical wormlike chains. 3. Translational friction coefficient. *Macromolecules* **12**, 32–38 (1979).
39 Barrett, A. J. Investigation of moments of intrachain distances in linear polymers. *Macromolecules* **17**, 1561–1566 (1984).
40 Yamakawa, H. & Yoshizaki, T. Effects of fluctuating hydrodynamic interaction on the hydrodynamic-radius expansion factor of polymer chains. *Macromolecules* **28**, 3604–3608 (1995).